0026-895X/02/6204-817–827$7.00
MOLECULAR PHARMACOLOGY
Vol. 62, No. 4
1764/1013765
Mol Pharmacol 62:817–827, 2002
Printed in U.S.A.

Desensitization of Homomeric α1 Glycine Receptor Increases with Receptor Density

PASCAL LEGENDRE, EMILIE MULLER, CARMEN IONELA BADIU, JOCHEN MEIER,[1] CHRISTIAN VANNIER, and ANTOINE TRILLER

Unité Mixte Recherche Centre National de la Recherche Scientifique 7102, Université Pierre et Marie Curie, Paris, France (P.L., E.M., C.I.B.); Institut National de la Santé et de la Recherche Médicale U497, Ecole Normale Supérieure, Paris, France (J.M., C.V., A.T.)

Received March 28, 2002; accepted July 12, 2002

This article is available online at http://molpharm.aspetjournals.org

ABSTRACT

Variations in the number of receptors at glycinergic synapses are now established and are believed to contribute to inhibitory synaptic plasticity. However, the relation between glycine receptor (GlyR) kinetics and density is still unclear. We used outside-out patch-clamp recordings and fast-flow application techniques to resolve fast homomeric GlyRα1 kinetics and to determine how the functional properties of these receptors depend on their density and on the presence of the anchoring protein gephyrin. The expression of GlyRs in human embryonic kidney cells increased with time and was correlated with an increase in GlyR desensitization at 2 days after transfection. Cotransfection of homomeric GlyRα1 bearing the gephyrin-binding site with gephyrin also increased desensitization but at 1 day after transfection compared with transfections of homomeric GlyRα1 without gephyrin. This increase results from the occurrence of a fast desensitization component and short applications of a saturating concentration of glycine suffice to promote a rapidly entered desensitized closed state. The level of desensitization changed neither the EC_{50} value nor the Hill coefficient of the glycine dose-response curves because the amplitude of the current was measured at the peak of the responses. These results demonstrate that variations in GlyR density during cluster formation result from a change in GlyR efficiency due to modifications in their desensitization properties.

Most ionotropic neurotransmitter receptors are clustered in the postsynaptic membrane. This is essential for effective synaptic transmission. Postsynaptic receptor cluster formation and stabilization requires intracellular molecular partners which form a subsynaptic protein scaffold and provide links to the cytoskeleton (Kneussel and Betz, 2000). Confinement of receptors in clusters increases receptor interaction, but little is known about how receptor density affects their functional properties.

Clustering of postsynaptic receptors at synapses is reversible. Active removal of GluR1 and GluR2 from glutamatergic synapses occurs during long-term depression (Luthi et al., 1999; Carroll et al., 1999). In contrast, GluR1 or GABAA receptor are rapidly inserted at glutamatergic or at GABAergic synapses, respectively, during long-term potentiation (Nusser et al., 1998; Hayashi et al., 2000). These processes have been proposed to result mainly from the internalization of the receptors or their insertion into the membrane. An alternative route for the progressive accumulation of receptors during synapse formation consists of the trapping of laterally diffusing receptors as shown for highly mobile extrasynaptic acetylcholine receptors during development of muscular synapses (Burden, 1998) and glycinergic synapses (Meier et al., 2001).

Glycine is the principal inhibitory neurotransmitters in spinal cord and brainstem The glycine receptor (GlyR) is composed of α_{1-4} and β subunits (for review, see Legendre, 2001). These subunits can form homomeric (5α subunits) or heteromeric complexes with 3α and 2β subunits (Legendre, 2001), the β subunit bearing the binding site for the anchoring protein gephyrin (Meyer et al., 1995). Trapping of GlyRs by the anchoring protein gephyrin after membrane insertion is fast and reversible (Meier et al., 2001; Rosenberg et al., 2001). This mechanism implies that the number of GlyRs within a cluster depends on a dynamic equilibrium between the number of trapped GlyRs and the number of escaping GlyRs. This observation also suggests that some GlyRs exist outside clusters. Differences in GlyR kinetics depending on receptor density seem likely to affect glycine receptor function in both immature and mature brain. Interestingly, extrasynaptic GlyRs can be activated both by spillover of glycine from adjacent synapses (Faber and Korn, 1988) and by nonsynaptic release of taurine, in both immature animals

This work was supported by Institut National de la Santé et de la Recherche Médicale, Centre National de la Recherche Scientifique, Ministère de la Recherche, and Université Pierre et Marie Curie.

[1] Current address: Developmental Physiology, Johannes-Müller Institute, Humboldt University Medical School (Charité), Berlin, Germany

ABBREVIATIONS: GluR, glutamate receptor; GlyR, glycine receptor; DPT, days post-transfection; HEK, human embryonic kidney; GFP, green fluorescent protein; PBS, phosphate-buffered saline.

and adults (Flint et al., 1998; Hussy et al., 2001). It is therefore important to determine how kinetics of currents at GlyRs varies as a function of their density, which is greater at synaptic than at nonsynaptic sites.

The apparent affinity (EC_{50}) of the GlyR for glycine changes when receptor expression in transfected oocytes is increased (Taleb and Betz, 1994). However, EC_{50} may fluctuate due to several mechanisms, including changes in ligand-binding affinity, modifications of channel efficacy (Colquhoun 1998), or changes in the desensitization properties of the receptor. Moreover, difficulties in resolving fast response components can introduce considerable errors into kinetic analysis of whole-cell currents. To overcome these problems, we have analyzed the kinetics of GlyRs in outside-out currents using fast-flow application techniques (Legendre, 1998). Outside-out patches were obtained from cultured HEK cells cotransfected with GlyRs and gephyrin, or from HEK cells transected with GlyRs alone. GlyR kinetics were analyzed at 1 and 2 days post-transfection (DPT).

Materials and Methods

Cell Culture and Transient Protein Expression. Human embryonic kidney (HEK) 293 cells were grown on glass coverslips in Dulbecco's modified Eagle's medium containing 10% fetal calf serum (Invitrogen, Carlsbad, CA) at 37°C and 7.5% CO_2. HEK cells were transfected 24 h after plating at 70% confluence using the calcium phosphate method and then incubated for 24 or 48 h to allow transient protein expression. cDNAs encoding an α1 subunit, an α1-βgb subunit and gephyrin-GFP chimera, were obtained as described previously (Meier et al., 2000). α1-βgb subunit bears the gephyrin-binding site in the M3–M4 intracellular domain (Meier et al., 2000). In both α1 subunits, a myc tag was located in the N terminus of the protein (Meier et al., 2000). In the following, myc-tagged subunits will be referred to as GlyRα1 and GlyRα1-βgb, respectively.

Fluorescence Microscopy. For immunofluorescence staining of receptor subunit, only cell-surface antigen was examined. It was revealed on unfixed cells at 0 to 2°C. For this purpose, transfected cells were incubated for 30 min on ice with mouse anti-myc antibody (clone 9E10; Roche Diagnostics, Mannheim, Germany) at a concentration of 5 μg/ml in phosphate-buffered saline (PBS) containing 2 mg/ml bovine serum albumin, 0.5 mM $CaCl_2$, and 0.5 mM $MgCl_2$. After extensive washing with PBS, cells were fixed for 15 min in 4% (w/v) paraformaldehyde in PBS. Fixed cells were washed in PBS and incubated with carboxymethyl indocyanine-3–conjugated, affinity-purified goat anti-mouse IgG (Jackson Immunoresearch Laboratories, West Grove, PA) at 5 μg/ml in PBS containing 0.12% (w/v) gelatin for 45 min at room temperature. Images were taken using the 63×/1.32 objective of a Leica DMR fluorescence microscope. GFP fluorescence was detected using an fluorescein isothiocyanate filter set.

Images were taken using the 100× objective of a Leica inverted fluorescence microscope equipped with appropriate filters (carboxymethyl indocyanine-3 and GFP fluorescence), and recorded with a 16-bit charge-coupled device camera (MicroMAX, Princeton Scientific Instruments, Monmouth Junction, NJ). Areas of 2 × 2 pixels (0.07 μm^2) were used as a frame to measure fluorescence at the cell periphery (12.7 ± 0.6 measurements were done on each cell). Three sets of 10 cells each (three independent sets of experiments) were measured in each culture (α1 at 1 and 2 DPT, and α1-βgb + gephyrin at 1 DPT). The quantification was performed using Metamorph image analysis software (Universal Imaging Corporation, Downingtown, PA).

Immunofluorescence intensity values measured with the software are given in arbitrary units, from the lowest intensity detectable to the saturation level, which we avoided during the acquisition, by choosing an appropriate exposure time for all cells. These measurements were done on images from which a same background was subtracted: this background was estimated from immunofluorescence intensity values measured in the intercellular space. Representative parts of HEK cell membrane in each transfection condition were selected, enlarged to illustrate expression patterns of GlyR at the cell surface, then used to acquire immunofluorescence intensity profiles representative of these patterns.

Outside-Out Patch Clamp Recordings. Standard outside-out recordings (Hamill et al., 1981) were made under direct visualization (Nikon Optiphot microscope) from the HEK cells (M-cell). The cell culture was continuously perfused at room temperature (20°C) in a recording chamber (0.5 ml) with an oxygenated bathing solution (2 ml/min) containing 145 mM NaCl, 1.5 mM KCl, 2 mM $CaCl_2$, 1 mM $MgCl_2$, 10 mM glucose, and 10 mM HEPES, pH 7.3, with the osmolarity adjusted to 300 mOsM.

Patch clamp electrodes were pulled from thick-wall borosilicate glass with a resistance of 10 to 15 MΩ. They were fire-polished and filled with a solution containing 135 mM CsCl, 2 mM $MgCl_2$, 4 mM Na_3ATP, 10 mM EGTA, and 10 mM HEPES, pH 7.2. The osmolarity was adjusted to 290 mOsM. Outside-out patches were obtained by slowly pulling out the pipettes. The resistance of outside-out patches ranged from 2 to 10 GΩ. Currents were recorded using an Axopatch 1D amplifier (Axon Instruments, Union City, CA). Outside-out currents were filtered at 10 kHz using an eight-pole Bessel filter (Frequency Devices, Haverhill, MA), sampled at 50 kHz (Digidata 1200 interface; Axon Instruments) and stored on an IBM PC-compatible computer using pCLAMP software 6.03 (Axon Instruments).

Drug Delivery. Outside-out single channel currents were evoked using a fast-flow application system as described previously (Legendre, 1998). Drugs were dissolved in the same solution used to perfuse the preparation. Control and drug solutions were fed by gravity into the two channels of a glass θ tube (2-mm o.d.; Hilgenberg, Malsfeld, Germany). Applications were controlled by solenoid valves.

The tip diameter of the θ tube was 200 μm. One lumen of the tube was connected to a reservoir of control solution. The other lumen of the pipette was connected to five different reservoirs for application of different solutions using a manifold. Solution exchange was performed by rapidly moving the solution interface across the tip of the patch pipette, using a piezoelectric translator (model P245.30; Physics Instrument (Walbronn, Germany). Concentration steps of glycine lasting 1 to 1000 ms were applied every 5 to 20 s depending on the time needed for recovery of outside-out currents. The 20 to 80% exchange time (≤ 0.06 ms) was determined after rupturing the seal by monitoring the change in the liquid junction evoked by the application of a control solution diluted by 10% to the open tip of the patch pipette (Legendre, 1998). The theoretical limit to the speed of solution change was estimated using the method of Maconochie and Knight (1989) (for detailed analysis, see Legendre, 1998). With a patch electrode resistance >5 MΩ and a tip diameter <1 mm, the estimated 20 to 80% exchange time was found to be ≤0.08 ms.

Outside-Out Patch Current Analysis. Outside-out currents were filtered at 2 kHz and stored for off-line analysis using Axograph 4.2 software (Axon Instruments). The desensitization time constants of the currents evoked by glycine and the recovery time constants from desensitization were estimated by fitting the desensitization phase of the responses and the relative amplitude of the test pulses during paired-pulse experiments with a sum of exponential curves using a simplex algorithm (Legendre, 1998). The goodness of the multiexponential fit and the number of exponential curves needed to fit the response time course were estimated by comparing the standard squared error of the fits (Clements et al., 1998, Legendre, 1998).

For dose-response curve analysis, the normalized data were fitted with a Hill equation of the form $I/I_{1mM} = 1/1 + (EC_{50}/[glycine])^{n_H}$, where I/I_{1mM} is the normalized response amplitude, I_{1mM} is the amplitude of the response obtained by 1 mM glycine application, EC_{50} is the glycine concentration ([glycine]) producing 50% of the

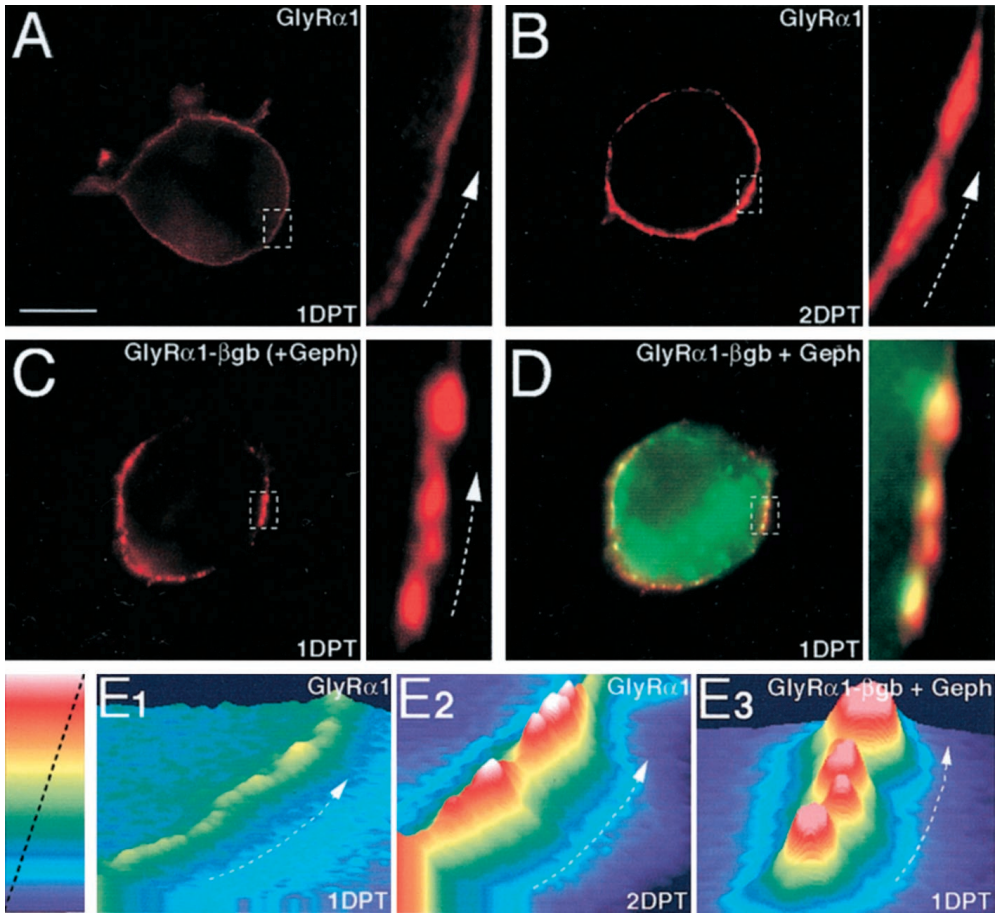

Fig. 1. Surface expression of myc-tagged GlyR α1 and α1-βgb subunits in HEK cells. The expression pattern of myc-tagged GlyR α1 subunits transfected alone at 1 and 2 DPT (A and B, respectively) and GlyR α1-βgb subunits cotransfected with gephyrin-GFP chimera at 1 DPT (C) was analyzed by myc-immunofluorescence staining of the cell surface (red). Cotransfection of gephyrin-GFP chimera is shown in green (D, superimposed image). Part of HEK cells membranes, in each condition of transfection (A-D), are represented at high magnifications (dotted lines). At 1 DPT, HEK cells transfected with GlyR α1 alone show a weak diffuse surface expression (A) that increases and becomes more irregular although still diffuse at 2 DPT (B). On the contrary, the cotransfection of GlyR α1-βgb with gephyrin-GFP leads to the formation of GlyR α1-βgb clusters (C), which are clearly colocalized with the gephyrin-GFP aggregates as illustrated by the superimposed image in D. Fluorescence intensity profiles (E1, E2, E3) obtained from HEK cell membrane magnifications of A, B, and C, respectively, are representative of each GlyR expression pattern described above. Diffuse patterns when GlyRα1 expressed alone, are represented by a constant fluorescence intensity along the membrane, higher at 2 DPT (E2) than at 1 DPT (E1), whereas the clustered pattern of GlyRα1-βgb cotransfected with gephyrin is represented by hot spots of fluorescence (E3). Scale bar for immunofluorescence intensity is done in arbitrary units. Dotted arrows indicate the correspondence between each image and its intensity profile. Scale bar (A-D), 10 μm; (higher magnifications) 3.51 μm.

maximum response and n_H is the Hill coefficient. Results are presented as mean $\pm$ S.D. throughout unless noted otherwise.

Results

To determine whether the density of GlyR molecules at the cell membrane influences the functional properties of these receptors, changes in receptor density with time after transfection were first analyzed by immunohistochemistry in cells at 1 and 2 DPT. These data were then compared with those obtained on cells cotransfected with GlyR and gephyrin. GlyR containing α1 subunits (GlyRα1) were used because this α subunit is present in the mature form of the post synaptic receptor (for review, see Legendre, 2001). We used homomeric GlyRα1 because after cotransfection, a pure population of heteromeric GlyRα/β incorporated within the cell membrane cannot be obtained convincingly for GlyRs. At best, the cells expressed a variable mixture of homomeric GlyRα1 and heteromeric GlyRα1/β (data not shown). To overcome this problem, we examined how interactions between the anchoring gephyrin and GlyRs affect receptor kinetics using a chimeric GlyR-α1 subunit (GlyRα1-βgb) bearing the β-subunit gephyrin-binding site in the M3–M4 intracellular domain (Meier et al., 2000). To ensure that the functional properties of GlyRs were not modified by insertion of the gephyrin-binding site in the M3–M4 intracellular domain of the α1 subunit, receptors with α1 subunit or with α1-βgb subunit without gephyrin were compared.

Expression Level in the Cell Membrane of Homomeric GlyRα1 in HEK Cells. The expression level of the tagged GlyR α1 and α1-βgb subunits was analyzed after transfection by myc-immunostaining (for GlyRs) and GFP-fluorescence (for gephyrin) on HEK cells, using fluorescence microscopy. At 1 DPT, GlyRα1 transfected alone had a diffuse pattern at the plasma membrane (Fig. 1A) without evidence of receptor clusters. Staining was more intense and irregular at 2 DPT although isolated GlyR aggregates were not observed (Fig. 1B), suggesting that GlyR density was increased at this stage. The expression pattern of GlyR α1-

βgb transfected alone was identical to that observed for GlyRα1 at 1 DPT and 2DPT (Meier et al., 2000).

Fluorescence intensity profiles corresponding to high magnification of HEK cells membranes in each condition of transfection shown in Fig. 1 (E1, E2, and E3 correspond to A, B. and C, respectively) are representative of the patterns described above. Therefore, the diffuse patterns observed for GlyRα1 transfected alone at 1 and 2 DPT are represented by a constant fluorescence intensity along the membrane, but higher at 2 DPT (E2) than at 1 DPT (E1). In contrast, the fluorescence intensity profile of clustered GlyRα1-βgb exhibited fluorescence hot spots (E3), corresponding to membrane GlyRα1-βgb clusters colocalized with gephyrin-GFP aggregates. However, when GlyRα1-βgb was cotransfected with gephyrin-GFP, isolated clusters were observed at the cell surface at 1 DPT (Fig. 1C) and were clearly colocalized with gephyrin-GFP aggregates (superimposed image, Fig. 1D). These results indicate that the cotransfection of gephyrin could induce the clustered surface expression of GlyRα1-βgb, which was not observed when GlyRα1-βgb was transfected alone. In addition, aggregates of gephyrin-GFP with various sizes were scattered in the cytoplasm, and when cells were permeabilized (data not shown), the aggregates were also stained for GlyRα1βgb-myc–associated IR (Meier et al., 2000). Fluorescence intensity profiles corresponding to high magnification of HEK cells membranes in each condition of transfection (Fig. 1; E1, E2, and E3 corresponding to A, B, and C, respectively) are representative of the patterns described above. Therefore, the diffuse patterns observed for GlyRα1 transfected alone at 1 and 2 DPT are represented by a constant fluorescence intensity along the membrane but higher at 2 DPT (E2) than at 1 DPT (E1). In contrast, the fluorescence intensity profile of clustered GlyRα1-βgb exhibited fluorescence hot spots (E3), corresponding to membrane GlyRα1-βgb clusters colocalized with gephyrin-GFP aggregates.

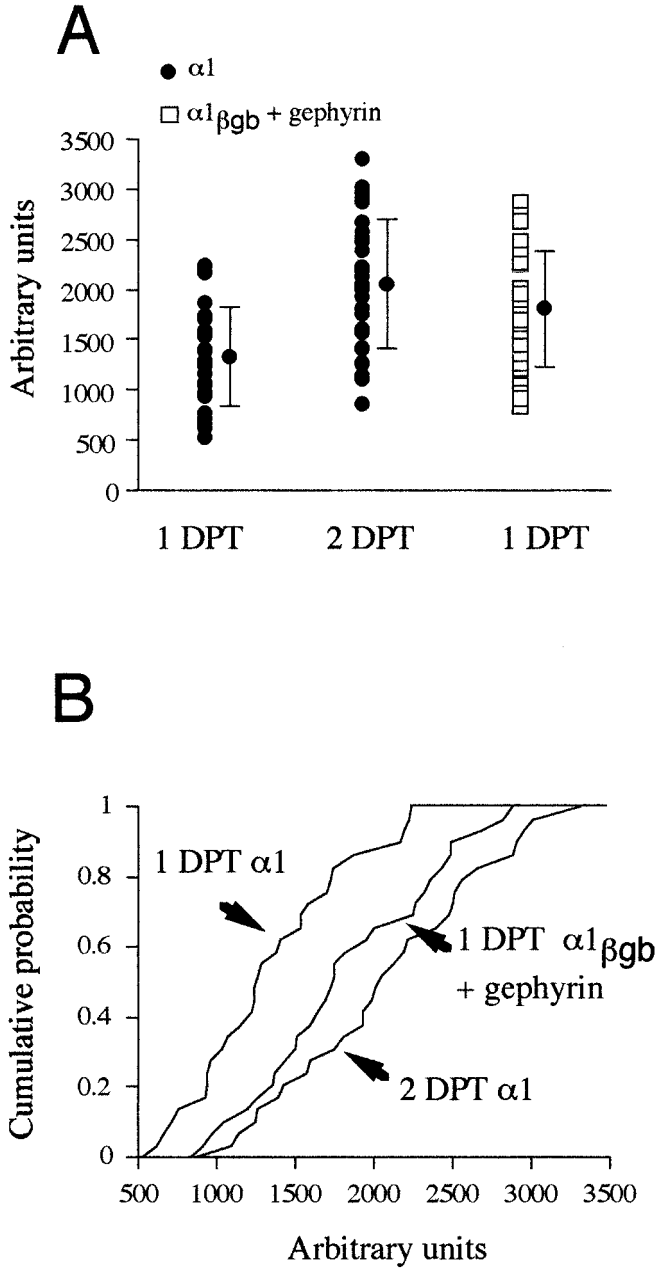

Fig. 2. Distribution of GlyR density. A, measurement of the immunofluorescence intensity (see *Materials and Methods*) at 1 DPT, 2 DPT on cells transfected with α1 (●) or at 1 DPT on cells cotransfected with α1-βgb and gephyrin (□). Averaged measurements (●) are represented as mean ± S.D. B, cumulative relative immunofluorescence intensity measurement distribution of data shown in E. Note that this distribution is shifted to the right at 2 DPT and that it is closely similar to the distribution obtained 1 DPT after cotransfection of α1-βgb and gephyrin. These two distributions are significantly different from that obtained at 1 DPT with homomeric GlyRα1 alone (Kolmogorov Smirnov test; $P < 0.05$).

To quantify changes in GlyR density, the fluorescence intensity per pixel for myc-immunostaining was measured at the cell periphery (see *Materials and Methods*). As shown in Fig. 2A, the fluorescence intensity per pixel varied from cell to cell. The mean fluorescence intensity per pixel increased from 1329 ± 484.4 ($n = 30$) to 2058 ± 640.8 ($n = 30$) at 1 DPT and 2 DPT, respectively. Gephyrin induced the formation of GlyRα1-βgb clusters. The mean immunofluorescence per pixel of these clusters was 1811 ± 570.8 ($n = 30$), a value 27% above that seen at 1 DPT when GlyRα1 expression was diffuse. The cumulative distribution of the mean fluorescence intensity per cell (Fig. 2B) increased significantly at 2 DPT for GlyRα1 alone or when GlyRα1-βgb was cotransfected with gephyrin (Kolmogorov Smirnov test, $P < 0.05$). These results suggest that GlyRα1 receptor density when expressed alone increased from 1 to 2 DPT although GlyRs were not clustered. They also suggest that at 1DPT the local density of GlyR (within clusters) was increased when GlyRα1-βgb was cotransfected with gephyrin (Meier et al., 2000).

Desensitization Properties of GlyR Change with Time Post-Transfection or When α1-βgb Was Cotransfected with Gephyrin. Analysis of the time course of desensitization of outside-out currents were performed on responses to concentration steps of 1 to 10 mM glycine of duration 1 s. Only currents with a stable time course were analyzed. When GlyRα1-βgb was cotransfected with gephyrin at 2 or 1 DPT, the time course of desensitization for glycine-evoked responses was faster than that of responses obtained at 1 DPT when GlyR α1 alone was transfected (Fig. 3A and 4A). This is attributable to the occurrence of a fast desensitization component. (Fig. 3) that was not observed for responses with a desensitized current that did not exceed 35% of the peak current (measured at the end of the concentration step). At 1 DPT, the application of glycine to a patch with GlyRα1 alone evoked responses that did not desensitize

(4 of 36 patches). Responses with desensitized current representing ≈ 5% of the peak current (5 of 36 patches) had a time course characterized by a relatively fast (30–60 ms) small desensitized component with no clear slower component (data not shown).

At 1 DPT, desensitizing outside-out currents representing more than 10% of the peak current were characterized by a time course with two decay components. As shown in Fig. 3A, the time course of desensitization was best fitted with the sum of two exponential curves with time constants of 22.8 ± 14 ms and 412 ± 200 ms (n = 10). These two desensitization components represented 11 ± 9 and 22 ± 8% of the peak current, respectively (Fig. 3, C and D).

Analysis of the desensitization time course of outside-out currents at 2 DPT revealed the presence of three desensitization components (Fig. 3B). The desensitization time course was best fitted by the sum of three exponential curves with time constants τ_{des1}, τ_{des2}, and τ_{des3} of 5.1 ± 3.1, 47.5 ± 26, and 453 ± 185, respectively (n = 16) (Fig. 3C). The fast desensitization component (τ_{d1}) represented 40 ± 18% of the total current, whereas τ_{des2} and τ_{des3} represented 20 ± 9 and 18 ± 16% of the peak current, respectively (Fig. 3D). These results show that the increase in the amount of desensitized current was related to the presence of a fast desensitization component at increased levels of GlyR density. Similar results were obtained at 1 DPT, when GlyRα1-βgb was cotransfected with gephyrin. The desensitization time course of the outside-out current was also fitted by the sum of three exponential curves with time constants τ_{des1}, τ_{des2}, and τ_{des3} of 4.2 ± 2.1, 34.2 ± 17.6, and 574 ± 174 ms, respectively (n = 15). The fast desensitization component (τ_{d1}) represented 47 ± 15% of the total current, whereas τ_{d2} and τ_{d3} represented 15 ± 13% and 13 ± 5%, respectively.

The Amount of Desensitized Current Was Increased at 2 DPT for GlyRα1 or at 1 DPT for GlyRα1-βgb + Gephyrin. As a first step toward understanding how homomeric GlyR density influences receptor-channel kinetics, we analyzed desensitization of outside-out currents evoked by long (300–1000 ms) application steps of a saturating concentration of glycine (≥ 1 mM). Outside-out currents were recorded from patches pulled from HEK cells at 1 or 2 DPT. Analyses were performed on cells transfected with myc-tagged rat GlyRα1 subunit or with myc-tagged GlyRα1-βgb (Fig. 4).

At 1 DPT, currents evoked by 0.3- to 1-s application steps of 1 to 10 mM glycine displayed little or no desensitization compared with outside-out responses obtained at 2 DPT (Fig. 4A). The amplitude of the peak current varied from one patch to another (50–2000 pA; Vh = −50 mV) even when the patches were obtained from the same HEK cells (data not shown). However the mean peak amplitude of outside-out currents from patches with GlyRα1 alone increased significantly from 368 ± 269 pA (n = 36) to 909 ± 561 pA (n = 39) at 1 and 2 DPT, respectively (U test $P < 0.01$). When GlyRα1 was cotransfected with gephyrin, the mean peak amplitude of the outside-out responses was 653 ± 514 pA (n = 65) at 1 DPT.

Changes in the amount of desensitized current with DPT resulted largely from a fast (≈5 ms) desensitization component. The slow desensitization component (400–500 ms) had

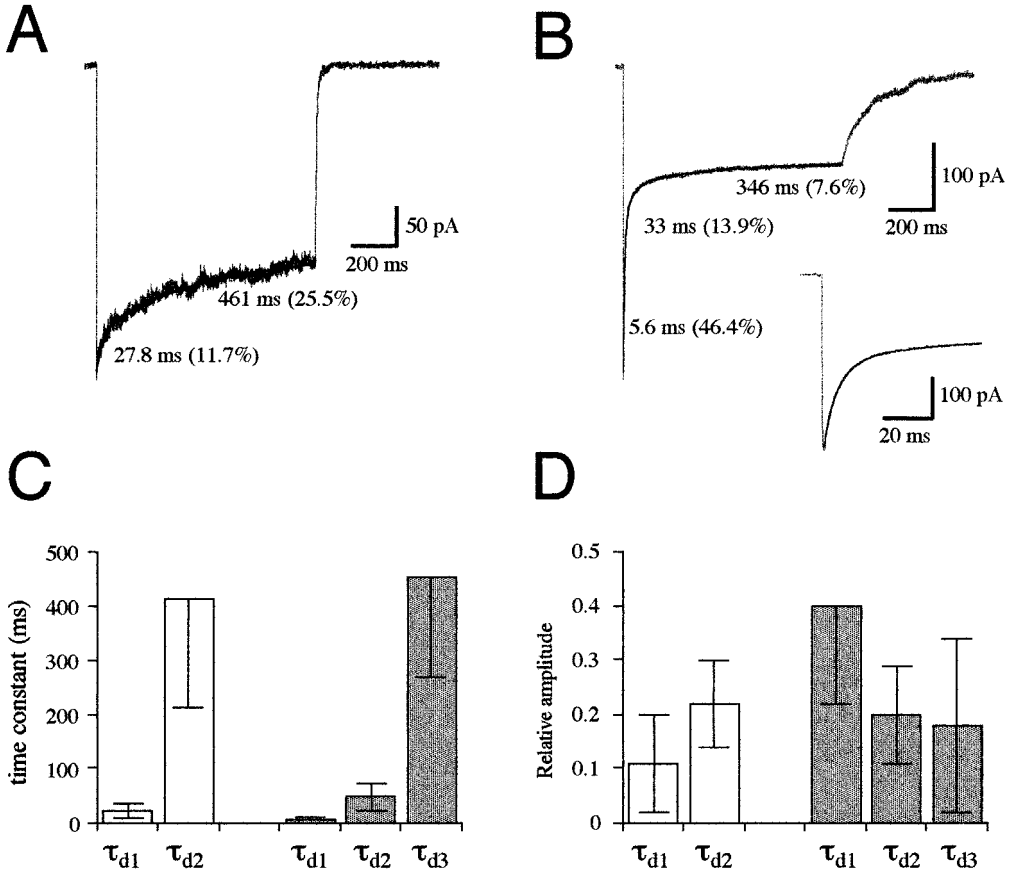

Fig. 3. Change in the desensitization time course of glycine-evoked current. A, example of current evoked by 1-s application of 3 mM glycine at 1 DPT from a patch with GlyRα1-βgb (Vh = −50 mV). Note that the desensitization time course can be fitted by the sum of two exponential curves. B, example of current evoked by 1-s application of 3 mM glycine at 1 DPT obtained from a patch with GlyRα1-βgb + gephyrin (Vh = −50 mV). This response shows a large desensitization with a complex time course fitted by the sum of three exponential curves. Inset, exponential fit of the onset of the desensitization time course at magnified time scale. C, average measurement of desensitization time constant obtained for poorly desensitizing current (□) and for current with a fast desensitization time course (▨). Note that the fast desensitization component obtained for highly desensitized current had an averaged time constant significantly lower (unpaired t test, $P < 0.01$) than the faster desensitization time constant measured for poorly desensitized current. On the contrary, the second desensitization components for highly desensitized currents had similar averaged time constant values than the than the faster desensitization time constant measured for poorly desensitized current (unpaired t test $P < 0.1$). D, histogram of the averaged relative amplitude to the peak current of desensitization components for poorly desensitized current (□) and for highly desensitizing currents (▨). Data are presented as mean ± S.D.

similar time constant and relative amplitude values at all DPT tested (Fig. 3). We quantified the level of desensitization of glycine-evoked currents by measuring the proportions of desensitized current at 300 ms after the beginning of the glycine application step. At 1 DPT, most currents obtained from GlyRα1 and GlyRα1-βgb patches displayed little desensitization, although there was some variation between patches (Fig. 4B). The proportion of desensitized outside-out current obtained from HEK expressing GlyRα1 or GlyRα1-βgb was not significantly different (U test; $P < 0.1$). The percentage of desensitized current for GlyRα1 and GlyRα1-βgb was 17.1 ± 12.9 (n = 21) and 20.6 ± 20.2% (n = 15), respectively. At 2 DPT, the proportion of desensitized current was 51.6 ± 21% (n = 15) and 45 ± 23% (n = 24) for GlyRα1 and for GlyRα1-βgb, respectively (Fig. 3B). These results suggest that GlyRα1 and GlyRα1-βgb have similar desensitization behaviors at 1 and 2 DPT. Data obtained from cells expressing GlyRα1 and GlyRα1-βgb were therefore pooled for further analysis. Both the GlyR expression level (Fig. 2) and the proportion of the desensitized current varied at 1 and 2 DPT (Fig. 3B), but their cumulative distributions (Fig. 4C) showed a significant increase in the proportion of desensitized current at 2 DPT (Kolmogorov Smirnov test; $P < 0.01$).

A similar effect was observed at 1 DPT when GlyRα1-βgb was coexpressed with gephyrin (see *Materials and Methods*). In these cells, glycine-evoked currents recorded from outside-out patches showed pronounced desensitization and the percentage of desensitized current was 55.3 ± 20.9% (n = 65). As for GlyR α subunits expressed alone, the proportion of desensitized current varied between patches (Fig. 4B). However, cumulative distributions of the percentage of desensitized current for GlyRα1-βgb + gephyrin and for GlyRα1 alone at 1 DPT were significantly different (Kolmogorov Smirnov test; $P < 0.01$). In contrast, distributions obtained at 2 DPT for glyRα1 alone and at 1 DPT for GlyRα1-βgb + gephyrin did not differ significantly (Fig. 4C).

Fast Desensitization Can Occur during 1-ms Application Step of 3 mM Glycine. A fast desensitization component implies that short applications of agonist (1 ms) may suffice to promote a rapid entry of channels into a desensitized closed state (Jones and Westbrook, 1995). This can be tested by paired-pulse experiments. Fast desensitization and its recovery was analyzed using short (1 ms) paired-pulse experiments with 3 mM glycine (Fig. 5). Paired pulses were applied at 0.1 Hz to allow full recovery of the outside-out current amplitude. Responses evoked by a 1-ms concentration step of 3 mM glycine had a fast 20 to 80% rise time. It was 0.21 ± 0.03 ms (n = 12) for currents displaying little desensitization (1 DPT) and 0.15 ± 0.04 ms (n = 16) for current with fast desensitization (2 DPT; 1 DPT GlyRα1-βgb + gephyrin).

At 1 DPT, for GlyRα1-βgb alone, desensitization had little or no effect on the amplitude of responses to currents evoked by short 3 mM glycine pulses (1 ms). In responses to paired glycine applications at variable intervals, the second application evoked a 21.3 ± 4.2% smaller peak current at 6-ms interval in 5 of 10 patches tested (Fig. 5A1). Recovery from desensitization was analyzed on data obtained from these five patches. The recovery time course was fitted with a single exponential curve (Fig. 5A2) with a time constant of 42.1 ± 22.5 ms (n = 5).

In contrast, desensitization significantly reduced the am-

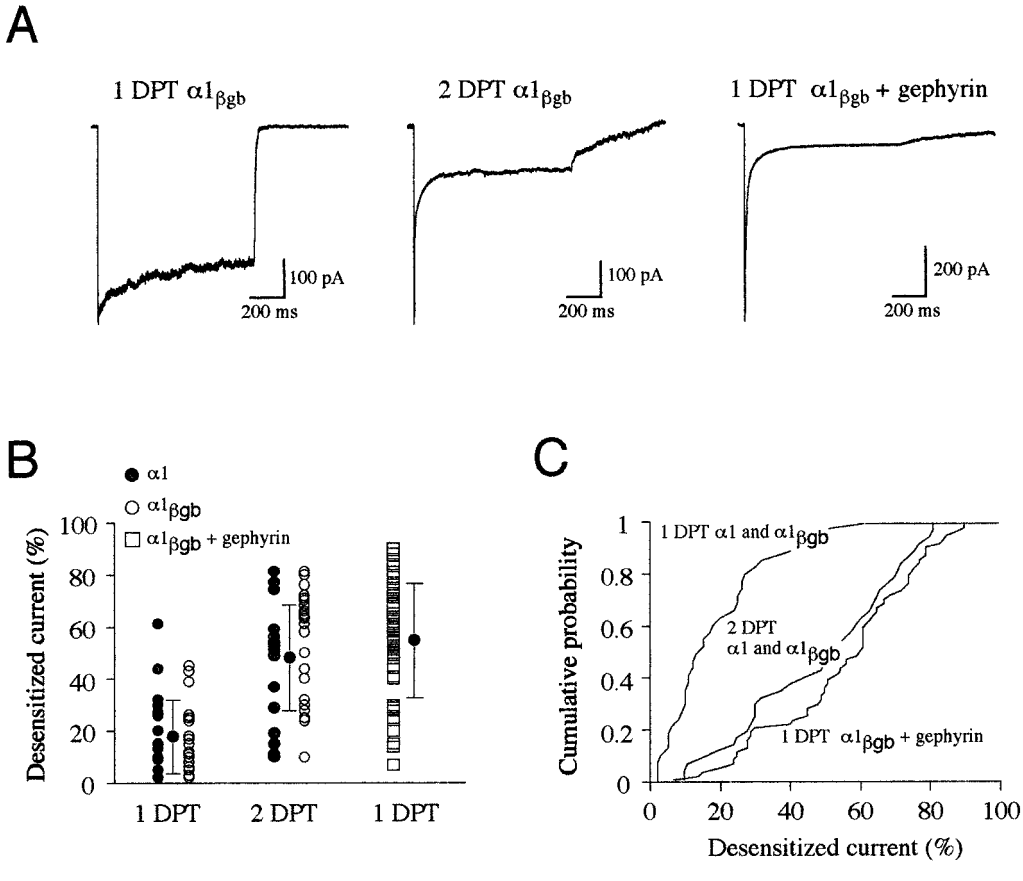

Fig. 4. Changes in the relative amplitude of the desensitizing current with DPT. A, examples of outside-out current evoked by 1-s application of 3 mM to a patch obtained from HEK cells 1 day after α1-βgb subunit transfection (left trace, 1 DPT), 2 days after transfection of α1-βgb subunit (middle trace, 2 DPT), and 1 d after cotransfection of α1-βgb and gephyrin (right trace, 1 DPT). All traces represent currents obtained from HEK transfected with chimeric α1 subunit α1-βgb bearing the binding site for gephyrin (Vh = −50 mV; 2-kHz cutoff frequency). Note the pronounced desensitizing current at 2 DPT and at 1 DPT when α1-βgb is cotransfected with gephyrin. B, measurement of the relative amplitude of the desensitizing current obtained at 1 DPT, 2 DPT on cells transfected with α1 (○) or α1-βgb (◉) and at 1 DPT on cells cotransfected with α1-βgb and gephyrin (□). Averaged measurements (●) are represented as mean ± S.D. C, cumulative percentage of desensitized current distribution of data shown in B. Data obtained with α1 and α1-βgb were pooled. Note that this distribution is shifted to the right at 2 DPT and that it is closely similar to the distribution obtained 1 DPT after cotransfection of α1-βgb and gephyrin. These two distributions are significantly different from that obtained at 1 DPT with homomeric GlyRα1 alone (Kolmogorov Smirnov test; $P < 0.01$).

plitude of chloride currents elicited by short glycine pulses (1 ms) at 1 DPT in experiments with cells coexpressing GlyRα1-βgb and gephyrin. Paired pulses at 6 ms interval resulted in a 91.1 ± 5.3% (n = 9) decrease in peak current (Fig. 5B1). For these patches, recovery from desensitization was well fitted by the sum of two exponential curves with time constants of 36.2 ± 23.5 and 158.6 ± 48.8 ms (n = 9) (Fig. 5B2). The relative amplitudes of these two components were 58.7 ± 21.3 and 51.3 ± 21.3% (n = 9), respectively. These results imply that the activation of GlyRα1-βgb + gephyrin by short agonist pulses promotes the rapid entry of receptor channels into desensitized states.

Decay Phase of Current Evoked by Short Concentration Step of Glycine. As shown in Figs. 5 and 6, responses with fast desensitization components also had a longer decay phase after glycine application. The decay of glycine-evoked currents was analyzed on responses to short applications (1 ms) of a saturating concentration of glycine (3 mM). At 1 DPT for GlyRα1 alone, the decay phase of the glycine-evoked currents was best fitted with the sum of two exponential curves (Fig. 6A) with time constants τ_1 and τ_2 of 6.2 ± 1.1 and 36.4 ± 15.5 ms (n = 10), respectively. τ_1 and τ_2 had relative amplitude of 68 ± 12.3 and 32 ± 12.3%, respectively. At 2 DPT for GlyRα1 or at 1 DPT for GlyRα1-βgb + gephyrin, the decay phase of the outside-out currents was best fitted with the sum of three exponential curves (Fig. 6B) with time constants τ_1, τ_2, and τ_3 of 3.3 ± 1, 18.2 ± 6.5, and 129 ± 53.8 ms, respectively (n = 14). τ_1, τ_2, and τ_3 had relative amplitudes of 36.7 ± 13.3, 38.2 ± 11.4, and 25.1 ± 11.5%, respectively (n = 14). This change in the time course of the decay phase and the occurrence of a long decay component can be directly related to GlyR desensitization as previously shown for rapidly desensitizing GABAA receptors (Jones and Westbrook 1995).

The initial part of the decay phase (τ_1 = 3.3 ms) of responses observed at 2 DPT for GlyRα1 or at 1 DPT for GlyRα1-βgb + gephyrin is likely to correspond to fast GlyR desensitization. As shown in Fig. 6C, the fast decay phase component of the response to 1-ms applications of glycine has a similar time course to that of the fast desensitization component of responses to long glycine pulses (1 s). Accordingly, the onset of the decay phase of the responses evoked by short glycine applications occurred before the end of the application step (Fig. 6D).

Recovery from Desensitization after Long Glycine Application Pulse. The slow desensitization component recovered slowly. Paired pulse experiments using a prepulse of 1 s (1 mM glycine) and test pulses of 50 ms applied at various intervals (Fig. 7) were performed to measure the recovery time constant of the slow desensitization component. Paired pulses were applied at 15-s intervals to ensure a complete recovery between paired applications. This analysis was performed on patches obtained from HEK cells cotransfected with GlyRα1-βgb and gephyrin (Fig. 7A). The recovery time course was analyzed using data from 10 different patches. The relative amplitude of the test pulses was estimated from the residual current measured at the end of responses to 1-s glycine applications. Outside-out currents with three desensitization components displayed a progressive recovery from desensitization. The recovery time course from desensitization was best fitted with the sum of three exponential components (Fig. 7B) with time constants τ_{r1}, τ_{r2}, and τ_{r3} of 37 ± 12, 185.4 ± 55, and 1040 ± 149 ms, respectively. τ_{r1}, τ_{r2}, and

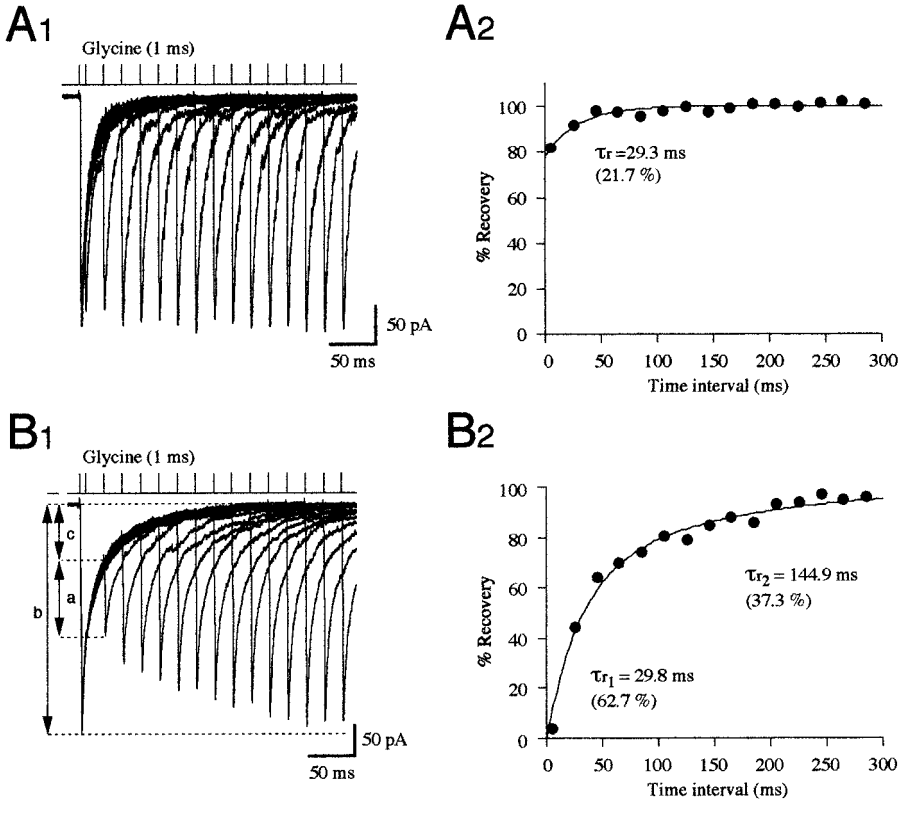

Fig. 5. Short application step of glycine and GlyR desensitization. A1, example of superimposed traces with little desensitization evoked by paired pulses of 3 mM glycine (1 ms) at 1 DPT with GlyRα1 alone (Vh = −50 mV). Interpulse intervals were 6, 26, 46, 66, 86, 106, 126, 146, 166, 186, 206, 226, 246, 266, and 286 ms. A2, data points were obtained from traces shown in A1. Note that paired pulses of glycine evoked a small desensitization with recovery time constant of ≈ 29 ms. B1, superimposed traces evoked by paired pulses of 3 mM glycine (1 ms) at 1 DPT with GlyRα1-βgb + gephyrin (Vh = −50 mV). B2, interpulse intervals were identical to those shown in A. Each data point represents individual measurement obtained on traces shown in B1. Note that paired pulses of glycine evoked a nearly complete desensitization of the transient current with the recovery time course being fitted with the sum of two exponential curves (time constants ≈30 ms and ≈145 ms). The relative decrease in the peak amplitude of the successive responses was estimated by dividing its amplitude (a) by the absolute amplitude value of the control response (b) minus the current baseline amplitude (c). The baseline current amplitude was measured just before the onset of the outside-out current evoked by the test pulse.

τ_{r3} had relative amplitudes of 23.2 ± 14.3, 44.8 ± 18.4, and 32 ± 8.8%, respectively.

Dose-Response Curve of Glycine-Evoked Responses and GlyR Desensitization. Estimates of EC_{50} and I_{max} from dose-response curves are subject to substantial error if the peak of the responses cannot be resolved due to fast desensitization. The fast-flow application technique can overcome this problem because it can resolve fast kinetics with a time course ≤0.1 ms. We estimated how desensitization affected dose-response measurements by measuring the amplitude of responses at the peak of the current and immediately after decay of the fast desensitization component. We also compared dose-response curves obtained from patches displaying fast or slow desensitizing currents.

Dose-response curves were obtained from responses to application of glycine pulses of 300-ms duration and concentrations ranging from 0.01 to 3 mM (Fig. 8). Two to five concentrations of glycine were usually tested with each patch, and response amplitudes were normalized to the peak current of the response obtained by the application of 1 mM glycine. EC_{50} and Hill coefficient values were obtained by fitting averaged data points with single binding isotherm functions (see *Materials and Methods*). Patches in which glycine-evoked currents showed a rundown or in which the desensitization time course changed substantially during the recording were excluded. For responses that showed little desensitization (1 DPT), fits to amplitudes measured from the peak of the response gave an EC_{50} of 73 μM and a Hill coefficient of 1.36 (Fig. 8C). Measuring the response amplitude at the end of the application step (300 ms) did not change EC_{50} or Hill coefficient values, resulting in an EC_{50} of 68 μM and a Hill coefficient of 1.36 (Fig. 7C).

Similar results were obtained for responses displaying fast desensitization (1 DPT, GlyRα1-βgb + gephyrin) when measurements were performed at the peak of the responses. The EC_{50} and Hill coefficient values were 73 μM and 1.43, respectively (Fig. 8D). However, when current amplitudes were measured at the end of the response, the

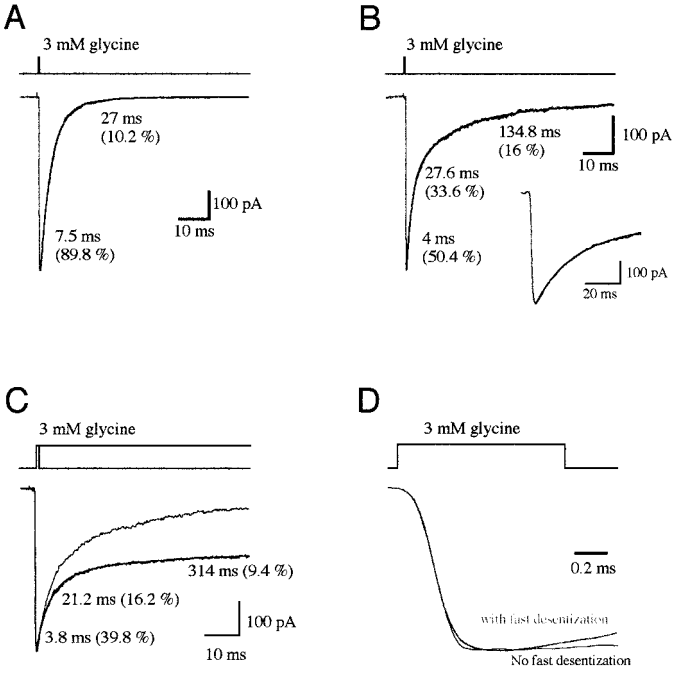

Fig. 6. Decay phase of the outside-out current evoked by 1 ms application of glycine. A, outside-out currents evoked by 1-ms application of 3 mM glycine on patches with GlyRs that did not display fast desensitization time-courses (gray) (Vh = −50 mV). The decay phase of this response was fitted with the sum of two exponential curves (line in black) with time constants of 7.5 ms and 27 ms. B, outside-out currents evoked by 1-ms application of 3 mM glycine on patches with GlyRs that display fast desensitization time-courses (gray trace) (Vh = −50 mV). The decay phase of this response was fitted with the sum of three exponential curves (line in black) with time constants of 4, 27.6, and 134.8 ms. Each trace shown in A and B is the average of five sweeps. C, superimposed traces of normalized current evoked by short (1 ms; black trace) and long (1 s; gray trace) application of 3 mM glycine. For display purpose, the first 100 ms of the recording were shown only. Note that fast desensitization time course of the response evoked by 1-s pulse of glycine can be well superimposed to the fast decay component of the response evoked by 1-ms pulse of glycine. In this example, the desensitization time course of the outside-out response evoked by 1-s application of glycine was fitted with the sum of three exponential curves (line in black) with time constants of 3.8, 21, and 314 ms. D, onset of normalized current shown in A (black trace) and B (gray trace). Note that the current declined before the end of the short glycine concentration step.

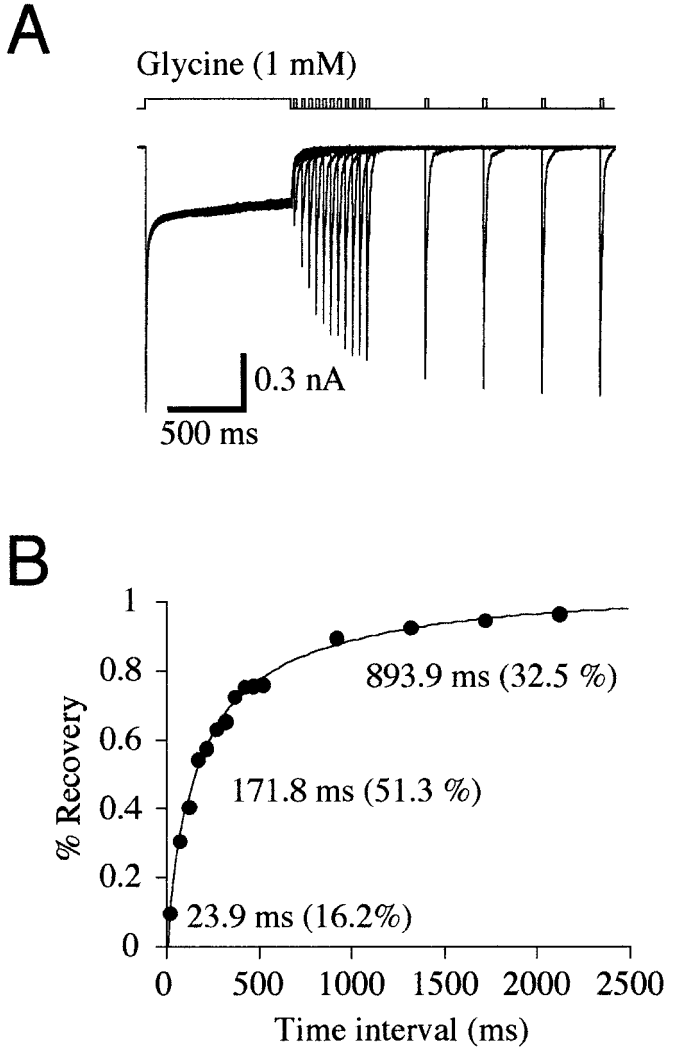

Fig. 7. Recovery from desensitization processes of current evoked by 1 sec application of glycine (1 mM). A, recovery from desensitization was analyzed by applying glycine (50 ms) at various intervals from the end of the 1-s concentration step (Vh = −50 mV). B, interpulse intervals were 20, 70, 120, 170, 220, 270, 320, 370, 420, 470, 520, 920, 1320, 1720, and 2120 ms. The time course of desensitization recovery for trace shown in A was fitted with the sum of three exponential curves with time constants of ≈24, ≈172, and ≈894 ms.

value determined for EC_{50} decreased and that for the Hill coefficient increased. The fit gave an EC_{50} of 34 μM and a Hill coefficient of 1.6. As shown in Fig. 8D, fast desensitization could influence the peak amplitude of outside-out responses evoked by >1 mM glycine, even during fast-flow applications. This presumably reflected the rapidly entered desensitized closed state during the fast activation phase of responses to saturating glycine concentrations (see Fig. 5). Thus, patches in which GlyRs displayed fast desensitization, the onset of the decay phase of responses to 1-ms pulses of glycine occurred before the end of the application step (Fig. 5D).

We could not estimate directly the relationship between glycine EC_{50} and the proportion of desensitizing currents, because it was difficult to obtain a full dose-response curve from a single outside-out patch. However, fluctuations in EC_{50} could be estimated from the S.D. of the normalized data points of dose-response curves. The fitting of the data points +S.D. and −S.D. measured at the plateau of the desensitizing current (see *Materials and Methods*) gave EC_{50} values ranging from 18 to 55 μM and Hill coefficient values varying between 1.27 and 2.7. EC_{50} and Hill coefficient measurements were less subject to fluctuation with data points obtained from the peak of responses or from those displaying little desensitization. In this case, EC_{50} and Hill coefficient values ranged from 62 to 77 μM and from 1.17 to 1.8, respectively. This implies that EC_{50} measurement can vary 3- to 4-fold, whereas the Hill coefficient can vary more than 2-fold depending only on whether or not the peak current can be resolved on desensitizing responses.

Discussion

In this article, we describe for the first time an increase in GlyR desensitization, in the absence of changes in apparent affinity, correlated with an increase in GlyR density. GlyRs desensitize more completely and more quickly at higher GlyR density, as observed in receptor clusters. Our results also provide experimental evidence accounting for the variations in EC_{50} and Hill coefficient values of homomeric GlyRs in transfected cells (Taleb and Betz, 1994; de Saint Jan et al., 2001).

The fast desensitization kinetics observed cannot result from the addition of the myc-tag amino acid sequence in the N terminus and they cannot be caused by the insertion of the binding site for gephyrin in the M3–M4 intracellular loop of the α1 subunit, because they were also observed for unmodified human homomeric GlyRα1 or GlyRα2 (de Saint Jan et al., 2001).

Peak Amplitude of Outside-Out Currents, Desensitization, and GlyR Density. Although it is not possible to directly measure distance between receptors, experimental arguments favor the hypothesis that this change in GlyR kinetics results from interactions between receptors caused by an increase in receptor density. Receptor desensitization increased with DPT and this increase paralleled an increase in the functional (peak current) and morphological (fluorescence intensity per pixel) density of receptor for GlyRα1 alone.

The averaged peak amplitude of outside-out currents increased between 1 and 2 DPT for GlyRα1 alone. A similar increase was observed when GlyRα1-βgb was cotransfected with gephyrin at 1 DPT. These observations suggest that the number of GlyR per patch increased at 2 DPT for GlyRα1 or at 1 DPT when GlyRα1-βgb was cotransfected with gephyrin. Accordingly, the mean intensity of fluorescence per pixel for mic-tagged GlyRα1 increased between 1 and 2 DPT or when GlyRα1-βgb was cotranfected with gephyrin. The peak amplitude of outside-out currents evoked by the application of

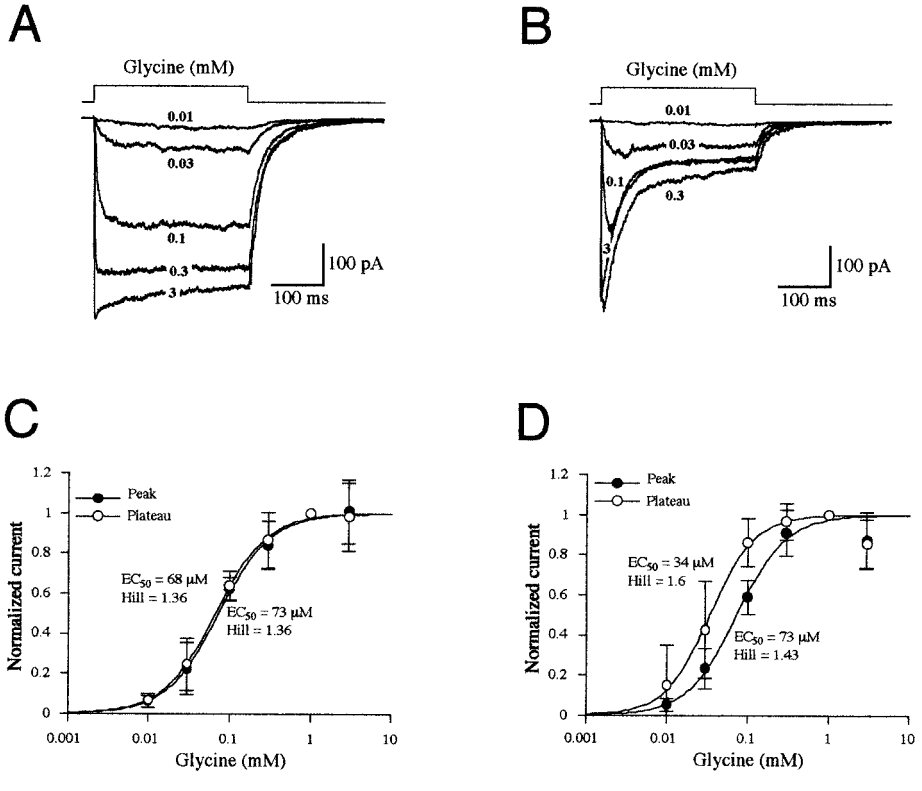

Fig. 8. Concentration response curves for glycine. A, responses of a patch at 1 DPT with GlyRα1 alone to fast-flow applications of different concentrations of glycine (Vh = −50 mV). The duration of the application was adjusted to obtain a steady-state amplitude of the currents. B, chloride currents evoked on a patch at 1 DPT with GlyRα1-βgb + gephyrin (Vh = −50 mV). Note that the amount of desensitized current depends on the glycine concentration. C, concentration response plot of data obtained in 15 patches at 1 DPT with GlyRα1 alone. Each point is the average of 7 to 15 measurements. Measurements were performed at the peak of the responses (●) and at the end of the application step (○). Data points were fitted with a single binding isotherm (see *Results*). Note that the fit of data points obtained at the peak of the response or at the end of the application of glycine gave closely similar EC_{50} and Hill coefficient values. D, concentration response plots of data obtained in 14 patches at 1 DPT with GlyRα1-βgb + gephyrin. Each point is the average of 6 to 14 measurements. Measurements were performed at the peak of the responses (●) and at the end of the application step (○). Data points were fitted with a single binding isotherm (see *Results*), with I_{max} being the amplitude of the current evoked by the application of 1 mM glycine. Note that EC_{50} and Hill coefficient values were decreased and increased, respectively, when measurements were performed at the end of the application step. Moreover, the amplitude of the responses evoked by the application of >1 mM glycine had a tendency to decrease at the peak current and at the plateau as well.

saturating glycine concentrations was highly variable between outside-out patches. Such variations seem unlikely to result from variations in the patch size alone, if it is assumed that variations in patch size are related to those in the input resistance of patch electrodes (10–15 MΩ). Effectively, the peak amplitude values of the outside-out currents were not normally distributed. Their mean−2 S.D. were lower than 0 and their coefficient of variation (CV = SD/mean) was larger than 61%. CV values at 1 DPT with GlyRα1, at 2 DPT with GlyRα1, and at 2 DPT with GlyRα1-βgb + gephyrin were 73, 61, and 78%, respectively. Accordingly, the variability in amplitude of currents recorded from outside-out patches seems likely to depend on other factors, including differences in density of receptors between patches.

αGlyRs Subunit Structure and Receptor Desensitization. Fast desensitization processes on a millisecond time scale have been described for some glutamate α-amino-3-hydroxy-5-methyl-4-isoxazolepropionic acid receptors (Jonas and Sakmann, 1992; Trussell et al., 1993; Mosbacher et al., 1994) and the process has been shown to depend on receptor subunit combination as well as on interactions between subunit amino acid domains (Koike et al., 2000; Partin, 2001; Robert et al., 2001). As for some α-amino-3-hydroxy-5-methyl-4-isoxazolepropionic acid (Trussell et al., 1993; Mosbacher et al., 1994) and $GABA_A$ receptors (Jones and Westbrook 1995), GlyR desensitization is fast enough to shape decay phase of response evoked by 1 ms pulse.

The occurrence of a fast desensitization process for aggregated homomeric GlyRs (5α1 subunits) contrasts with previous observations, also using fast application techniques, which described slower desensitization kinetics for neuronal heteromeric GlyRα1/β (Harty and Manis, 1998; Legendre, 1998). The incorporation of the β subunits in heteromeric GlyRs ($3\alpha_1/2\beta$) may modify desensitization properties of GlyRs through the interaction of the β subunits with α subunits. This hypothesis should be tested on heteromeric GlyRα/β. However, after cotransfection a pure population of heteromeric GlyRα/β incorporated within the cell membrane cannot be obtained convincingly for GlyRs.

The desensitization properties of homomeric GlyRs may reflect the stabilization of closed-state configurations resulting in an uncoupling of the binding domain from the gate of the pore involving the intracellular loop domains of the GlyR α subunits (Lynch et al., 1997). The observed changes in GlyR desensitization properties with receptor confinement might then depend on altered allosteric interactions between the α subunit protein domains and direct interactions with confined neighboring receptors. The two intracellular loops M1–M2 and M3–M4 of the α subunits have been suggested to regulate GlyR desensitization. Spontaneous mutations (P250T) and amino acid substitutions (W243A and I244A) within the M1–M2 intracellular loop of the alpha1 GlyR subunit are known to alter GlyR desensitization properties (Lynch et al., 1997; Saul et al., 1999). This loop links the transmembrane domains M1 and M2, which form the channel pore (for review, see Legendre, 2001). The M3–M4 intracellular loop of α subunits is also involved in controlling GlyR desensitization, at least for GlyRs containing α3 subunits. Two alternatively spliced transcripts, α3K and α3L, have been described, and GlyRs containing α3K subunits desensitize more rapidly than those composed of α3L subunits (Nikolic et al., 1998). This property results from the deletion of 15 amino acid residues in the intracellular loop linking the transmembrane domains M3 and M4 of the α3K transcripts. The M3–M4 intracellular domain of the α1 subunit has not been shown to control GlyR desensitization, but by interacting with the M1–M2 loop (Nikolic et al., 1998), this large GlyR intracellular loop may be involved in this process. Consequently, binding of gephyrin to GlyRα1-βgb might modify receptor desensitization kinetics. Accordingly, the binding of gephyrin to GlyRα1-βgb by changing the conformation of the M3-M4 intracellular loop could modify interactions with the M1–M2 intracellular domain, and so mimic the effect of GlyR density on receptor desensitization. Whatever the mechanism, receptor density and gephyrin binding effects on GlyR desensitization may well involve changes in the conformation of the intracellular loops.

Homomeric GlyR Density and Glycine EC_{50}. Our experiments show that the glycine EC_{50} value was independent of the expression density of homomeric GlyRs when response amplitudes were measured at the peak of the evoked outside-out current. This result seems to contradict previously published data from transfected oocytes showing that EC_{50} decreased at higher densities of GlyR expression (Taleb and Betz 1994). This change in the glycine EC_{50} values with GlyR expression level has been described previously using whole-cell intracellular recordings (Taleb and Betz, 1994). However, this type of experiment cannot resolve the true peak amplitude of glycine-evoked currents because of the slow kinetics of solution exchange relative to the time course of GlyR desensitization. The amplitude responses measured for desensitized currents lead to an underestimation of EC_{50} (Fig. 8). For similar reasons, the patch-to-patch variability in desensitized current amplitudes can account for cell-to-cell variations in the glycine EC_{50} value as reported for GlyRs expressed in oocytes (de Saint Jan et al., 2001) or HEK cells (Pribilla et al., 1992; Bormann et al., 1993; Lynch et al., 1997; Fucile et al., 1999; Moorhouse et al., 1999).

Our analysis also shows that estimates for the Hill coefficient may also be suspect if peak current amplitudes are masked by a rapid time course of desensitization. This might explain the relationship between the Hill coefficient and the expression level of GlyR derived from experiments in oocytes (Taleb and Betz, 1994). Estimates of the Hill coefficient for glycine, in experiments on homomeric GlyR, vary considerably between studies, with higher values reported in work based on chloride currents evoked in oocytes by slow glycine applications (for review, see de Saint Jan et al., 2001).

Functional Significance of the Density-Dependent GlyR Desensitization. Clusters of homomeric GlyRα have previously been described in mammalian neurons (Meier et al., 2000), and homomeric GlyRsα1 are activated in the zebrafish hindbrain by the release of a single synaptic vesicle (Legendre, 1997). The mechanism of homomeric GlyR aggregation at postsynaptic location remains unknown but it may result from homophilic interaction between GlyRs (Meier et al., 2000). Mechanisms of receptor clustering are complex and depend in part on synaptic activity (Kneussel and Betz, 2000). GlyR binding to gephyrin has recently been shown to be a reversible mechanism (Meier et al., 2001). Receptors in the plasma membrane can thus alternate between diffusive and confined states, with GlyR-gephyrin interactions controlling the proportion of receptors present in confined areas.

Our results give new functional significance to the hypoth-

esis that these dynamic properties affect regulation of the number of postsynaptic receptors, according to the concept of donor-acceptor synapse (Meier et al., 2001). Few nonclustered receptors exist at a given time (Meier et al., 2000) and any receptor may rapidly enter a diffusive state, resulting in rapid changes in desensitization properties. Unclustered receptors may then have different functions than synaptic receptors. They seem likely to be most effectively activated by glycine spillover from the synaptic cleft after repetitive presynaptic firing (Faber and Korn, 1988) resulting in a tonic inhibition with slower kinetics than that corresponding to activation of clustered synaptic GlyRs.

Acknowledgments

We thank Dr. Richard Miles for valuable help and discussions.

References

Bormann J, Rundstrom N, Betz H, and Langosch D (1993) Residues within transmembrane segment M2 determine chloride conductance of glycine receptor homo- and hetero-oligomers. *EMBO (Eur Mol Biol Organ) J* **12:**3729–3737.

Burden SJ (1998) The formation of neuromuscular synapses. *Genes Dev* **12:**133–148.

Carroll RC, Lissin DV, Vonz Astrow M, Nicoll RA, and Malenka RC (1999) Rapid redistribution of glutamate receptors contributes to long-term depression in hippocampal cultures. *Nat Neurosci* **2:**454–460.

Clements JD, Feltz A, Sahara Y, and Westbrook GL (1998) Activation kinetics of AMPA receptor channels reveal the number of functional agonist binding sites. *J Neurosci* **18:**119–127.

Colquhoun D (1998) Binding, gating, affinity and efficacy: the interpretation of structure-activity relationships for agonists and of the effects of mutating receptors. *Br J Pharmacol* **125:**924–947.

de Saint Jan D, David-Watine B, Korn H, and Bregestovski P (2001) Activation of human alpha1 and alpha2 homomeric glycine receptors by taurine and GABA. *J Physiol* **535:**741–755.

Faber DS and Korn H (1988) Synergism at central synapses due to lateral diffusion of transmitter. *Proc Natl Acad Sci USA* **85:**8708–8712.

Flint AC, Liu X, and Kriegstein AR (1998) Nonsynaptic glycine receptor activation during early neocortical development. *Neuron* **20:**43–53.

Fucile S, de Saint Jan D, David-Watine B, Korn H, and Bregestovski P (1999) Comparison of glycine and GABA actions on the zebrafish homomeric glycine receptor. *J Physiol* **517:**369–383.

Kneussel M and Betz H (2000) Receptors, gephyrin and gephyrin-associated proteins: novel insights into the assembly of inhibitory postsynaptic membrane specializations. *J Physiol* **525:**1–9.

Hamill OP, Marty A, Neher E, Sakmann B, and Sigworth FJ (1981) Improved patch clamp techniques for high-resolution current recordings from cells and cell free patches. *Pfleug Arch Eur J Physiol* **391:**85–100.

Harty TP and Manis PB (1998) Kinetic analysis of glycine receptor currents in ventral cochlear nucleus. *J Neurophysiol* **79:**1891–1901.

Hayashi Y, Shi SH, Esteban JA, Piccini A, Poncer JC, and Malinow R (2000) Driving AMPA receptors into synapses by LTP and CaMKII: requirement for GluR1 and PDZ domain interaction. *Science (Wash DC)* **287:**2262–2267.

Hussy N, Bres V, Rochette M, Duvoid A, Alonso G, Dayanithi G, and Moos FC (2001) Osmoregulation of vasopressin secretion via activation of neurohypophysial nerve terminals glycine receptors by glial taurine. *J Neurosci* **21:**7110–7116.

Jonas P and Sakmann B (1992) Glutamate receptor channels in isolated patches from CA1 and CA3 pyramidal cells of rat hippocampal slices. *J Physiol* **455:**143–171.

Jones MV and Westbrook GL (1995) Desensitized states prolong GABAA channel responses to brief agonist pulses. *Neuron* **15:**181–191.

Kneussel M and Betz H (2000) Receptors, gephyrin and gephyrin-associated proteins: novel insights into the assembly of inhibitory postsynaptic membrane specializations. *J Physiol* **525:**1–9.

Koike M, Tsukada S, Tsuzuki K, Kijima H, and Ozawa S (2000) Regulation of kinetic properties of GluR2 AMPA receptor channels by alternative splicing. *J Neurosci* **20:**2166–2174.

Legendre P (1998) A reluctant gating mode of glycine receptor channels determines the time course of inhibitory miniature synaptic events in zebrafish hindbrain neurons. *J Neurosci* **18:**2856–2870.

Legendre P (1997) Pharmacological evidence for two types of postsynaptic glycinergic receptors on the Mauthner cell of 52-h-old zebrafish larvae. *J Neurophysiol* **77:**2400–2415.

Legendre P (2001) The glycinergic inhibitory synapse. *Cell Mol Life Sci* **58:**760–793.

Luthi A, Chittajallu R, Duprat F, Palmer MJ, Benke TA, Kidd FL, Henley JM, Isaac JT, and Collingridge GL (1999) Hippocampal LTD expression involves a pool of AMPARs regulated by the NSF-GluR2 interaction. *Neuron* **24:**389–399.

Lynch JW, Rajendra S, Pierce KD, Handford CA, Barry PH, and Schofield PR (1997) Identification of intracellular and extracellular domains mediating signal transduction in the inhibitory glycine receptor chloride channel. *EMBO (Eur Mol Biol Organ) J* **16:**110–120.

Maconochie DJ and Knight DE (1989) A method for making solution changes in the submillisecond range at the tip of a patch pipette. *Pfleug Arch Eur J Physiol* **414:**589–596.

Meier J, Meunier-Durmort C, Forest C, Triller A, and Vannier C (2000) Formation of glycine receptor clusters and their accumulation at synapses. *J Cell Sci* **113:**2783–2795.

Meier J, Vannier C, Serge A, Triller A, and Choquet D (2001) Fast and reversible trapping of surface glycine receptors by gephyrin. *Nat Neurosci* **4:**253–260.

Meyer G, Kirsch J, Betz H, and Langosch D (1995) Identification of a gephyrin binding motif on the glycine receptor beta subunit. *Neuron* **15:**563–572.

Moorhouse AJ, Jacques P, Barry PH, and Schofield PR (1999) The startle disease mutation Q266H, in the second transmembrane domain of the human glycine receptor, impairs channel gating. *Mol Pharmacol* **55:**386–395.

Mosbacher J, Schoepfer R, Monyer H, Burnashev N, Seeburg PH, and Ruppersberg JP (1994) A molecular determinant for submillisecond desensitization in glutamate receptors. *Science (Wash DC)* **266:**1059–1062.

Nikolic Z, Laube B, Weber RG, Lichter P, Kioschis P, Poustka A, Mulhardt C, and Becker CM (1998) The human glycine receptor subunit alpha3. Glra3 gene structure, chromosomal localization and functional characterization of alternative transcripts. *J Biol Chem* **273:**19708–19714.

Nusser Z, Hajos N, Somogyi P, and Mody I (1998) Increased number of synaptic GABA(A) receptors underlies potentiation at hippocampal inhibitory synapses. *Nature (Lond)* **395:**172–177.

Partin KM (2001) Domain interactions regulating AMPA receptor desensitization. *J Neurosci* **21:**1939–1948.

Pribilla I, Takagi T, Langosch D, Bormann J, and Betz H (1992) The atypical M2 segment of the beta subunit confers picrotoxinin resistance to inhibitory glycine receptor channels. *EMBO (Eur Mol Biol Organ) J* **11:**4305–4311.

Robert A, Irizarry SN, Hughes TE, and Howe JR (2001) Subunit interactions and AMPA receptor desensitization. *J Neurosci* **21:**5574–5586.

Rosenberg M, Meier J, Triller A, and Vannier C (2001) Dynamics of glycine receptor insertion in the neuronal plasma membrane. *J Neurosci* **21:**5036–5044.

Saul B, Kuner T, Sobetzko D, Brune W and Hanefeld F, Meinck HM, and Becker CM (1999) Novel GLRA1 missense mutation (P250T) in dominant hyperekplexia defines an intracellular determinant of glycine receptor channel gating. *J Neurosci* **19:**869–377.

Taleb O and Betz H (1994) Expression of the human glycine receptor alpha 1 subunit in Xenopus oocytes: apparent affinities of agonists increase at high receptor density. *EMBO (Eur Mol Biol Organ) J* **13:**1318–1324.

Trussell LO, Zhang S, and Raman IM (1993) Desensitization of AMPA receptors upon multiquantal neurotransmitter release. *Neuron* **10:**1185–1196.

Address correspondence to: Dr. P. Legendre, UMR 7102 Neurobiologie des Processus Adaptatifs, Laboratoire de neurobiologie et neuropharmacologie de la synapse, Bât B. 6ème étage, boîte 8, Université Pierre et Marie Curie, 7 Quai Saint Bernard, 75252 Paris Cedex 05, France. E-mail: pascal.legendre@snv.jussieu.fr